Ductility of Filled Polymers

S. BAZHENOV, J. X. LI, A. HILTNER,* and E. BAER

NASA-CCDS on Materials for Space Structures and the Center for Applied Polymer Research, Case Western Reserve University, Cleveland, Ohio 44106

SYNOPSIS

The ductility of a calcium carbonate-filled amorphous copolyester PETG in a uniaxial tensile test was examined as a function of the filler volume fraction. A ductile-to-quasi-brittle transition occurred as the volume fraction of filler increased. This transition was from propagation of a stable neck through the entire gauge length of the specimen to fracture in the neck without propagation. The draw stress (lower yield stress) did not depend on the filler content and was equal to the draw stress of the unfilled polymer. It was therefore possible to use a simple model to predict the dependence of the fracture strain on the filler volume fraction. It was proposed that when the fracture strain decreases to the draw strain of the polymer the fracture mechanism changes and the fracture strain drops sharply. The critical filler content at which the fracture mode changes is determined primarily by the degree of strain-hardening of the polymer. © 1994 John Wiley & Sons, Inc.

INTRODUCTION

Polymers filled with rigid inorganic particles display higher values of Young's modulus and better thermostability than do unfilled polymers. Unfortunately, the filler also leads to reduction of the fracture strain.[1-6] For calcium carbonate-filled high-density polyethylene (HDPE), at filler fractions less than 15 vol %, the deformation is ductile, much like the unfilled polymer.[4] With further increase in filler content, the fracture strain sharply drops at a filler fraction (V_f) of approximately 20 vol %.[4] At V_f > 30 vol %, the fracture is brittle and the fracture strain is practically independent of filler content. Similar behavior, characterized by a sharp drop of fracture strain in a comparatively narrow interval of filler content, is observed for filled polypropylene.[3]

When a transition in the fracture mode occurs with a sharp drop in the fracture strain, it is usually described as a ductile-to-brittle transition. However, the "brittle" fracture of filled polyethylene is accompanied by localized ductile yielding in thin crazelike structures, where the local elongation of the matrix reaches the fracture elongation of the unfilled polymer (400–800%) while the overall elongation is only 3–5%.[7] Hence, this transition in filled polymers is more accurately described as a ductile-to-quasi-brittle one.

The critical filler content (V_f^*) of the ductile-to-quasi-brittle transition depends on the particle properties such as surface treatment[8-10] and size.[11-14] However, the effect of matrix properties on V_f^* is even more significant and V_f^* varies widely from one polymer to another. For example, V_f^* is less than 5 vol % in poly(vinyl chloride) (PVC)[15]; V_f^* = 10–15 vol % in polypropylene (PP); $V_f^* \approx 20$ vol % in HDPE[4,14]; and $V_f^* > 55$ vol % in rubber.[16] Furthermore, the critical filler volume fraction in HDPE increases from 20 to 40 vol % when the molecular weight is raised from 40,000 to 1,000,000.[14]

A number of attempts have been made to analytically model the effect of rigid filler particles on fracture stress and strain. Smith studied the condition for particle debonding in filled rubber, which is the initial failure event. He showed that the debonding strain (e_f) is given by the following equation[16]:

$$e_f = e_m(1 - \beta V_f^{1/3}) \quad (1)$$

where e_m is a constant; V_f, the volume fraction of the filler; and β, a geometric factor determined by

* To whom correspondence should be addressed.

Journal of Applied Polymer Science, Vol. 52, 243–254 (1994)
© 1994 John Wiley & Sons, Inc. CCC 0021-8995/94/020243-12

the particle packing and shape assumed. To obtain eq. (1), Smith introduced a model in which the composite was described by a cubic array of close-packed spherical particles for which $\beta = 1.105$.

This approach was extended by Nielsen to fracture of filled polymers with the assumption that the polymer follows Hooke's relationship between the stress and the strain.[17,18] For simplicity, a cubic array of cubic particles was used. Then, for well-bonded particles, the expression for fracture strain is analogous to eq. (1):

$$\varepsilon_f = \varepsilon^*(1 - \beta V_f^{1/3}) \quad (2)$$

where ε_f and ε^* are the fracture strain of filled and unfilled polymer, respectively, and β for the case of cubic particles is equal to 1.0.[17,18]

Nielsen further considered the case when the particles are debonded from the polymer. Assuming that the crack passes through the voids formed by debonding, a "two-thirds" power dependence of the fracture stress on the particle volume fraction was derived:

$$\sigma_f = \sigma^*(1 - \beta V_f^{2/3}) \quad (3)$$

where σ^* is the strength of the unfilled polymer. Equation (3) also describes the yield stress if the particles are debonded before yielding.[6] If adhesion is better, and debonding occurs as a result of yielding, the yield stress is constant and equal to the yield stress of the matrix. The fracture stress predicted by eq. (3) is generally in good agreement with experimental data. Examples are filled PP and PE.[1,5,6]

Nielsen also developed a numerical solution for the fracture strain of a filled polymer with debonded particles that predicts a fracture strain that is always higher than that with well-bonded particles.[18] The fracture strain of filled PE and PP is usually lower than either eq. (2) or the numerical solution for debonded particles. In addition, the shape of the experimental dependence of fracture strain on V_f is different from that described by either solution. Both solutions predict a continuous decrease in fracture strain that is most rapid at low filler contents with a smooth reduction as V_f increases. The actual dependence of the fracture strain on V_f for PE and PP is qualitatively different: An initial moderate reduction in fracture strain at low filler contents is followed by a sharp drop in fracture strain[3,4] at the transition from ductile-to-quasi-brittle fracture.

To determine the fracture strain, Nielsen assumed Hooke's relationship between stress and strain, which is reasonable for filled rubber.[16] It is not surprising that the fracture strain of polymers such as PE and PP, which deform by localized neck formation and propagation and have essentially non-Hookean behavior, has a different dependence on filler volume fraction from that predicted by Nielsen.

In light of the discrepancy between theory and experimental data, the goal of the present study was to develop an approach that would take into account the effect of necking on the fracture strain of filled polymers. In particular, the intent was to study the critical condition for the transition from ductile-to-quasi-brittle fracture and to determine the most important properties of the matrix that determine the transition.

EXPERIMENTAL

The matrix polymer was Kodar 6763 (PETG), an amorphous copolyester from Eastman Kodak. The filler was Camel-WITE, calcium carbonate from Genstar Stone. The cubic-shaped particles varied in size from 0.5 to 13 μm with an average particle size of 2.2 μm (Fig. 1).

The polymer and filler were blended in a Brabender Banbury mixer at 200°C for 10 min, then compression-molded into 2.0 mm-thick plaques at 200°C and 450 psi pressure for 5 min followed by water cooling of the mold. The tensile properties of dog-bone specimens cut to the ASTM D 1708 geometry were determined using an Instron testing machine at a speed of 2 mm/min. Four specimens of each composition were tested and the results averaged. Four compositions with the weight fractions of the filler equal to 5, 15, 30, and 50 wt % were studied. Converted into volume fractions, the filler contents were equal to 2.4, 7.2, 14, and 24 vol %, respectively.

The fractured specimens were photographed with a Nikon FM2 camera. The necked region was subsequently fractured in liquid nitrogen parallel to the draw direction in order to reveal the internal morphology. The cryogenic fracture surfaces were coated with 90 Å of gold and examined in the JEOL JSM-840A scanning electron microscope (SEM).

RESULTS AND DISCUSSION

Failure Behavior

Figure 2 shows typical engineering stress–strain curves for unfilled PETG and PETG filled with $CaCO_3$. The character of the curves changed with

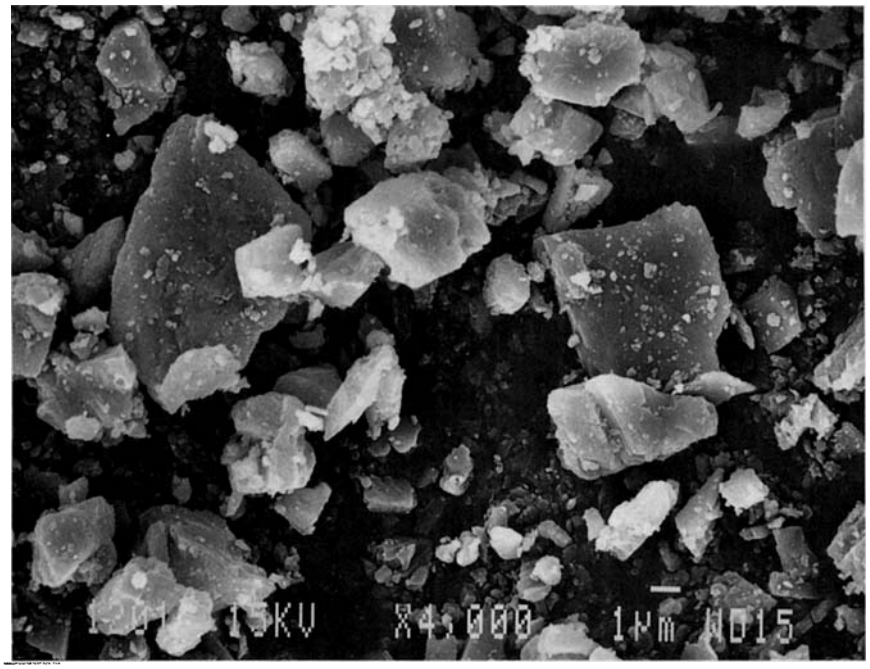

Figure 1 SEM micrograph of calcium carbonate particles.

an increase in the filler content. The stress–strain curve of unfilled PETG was typical of ductile polymers. After reaching the yield point, the stress dropped to the lower yield stress or draw stress (σ_d) and remained constant while the neck propagated through the entire gauge length of the specimen. This was followed by a region of strain-hardening where the stress gradually increased as the necked material extended uniformly. In the strain-hardening region, the increase in stress was linear with

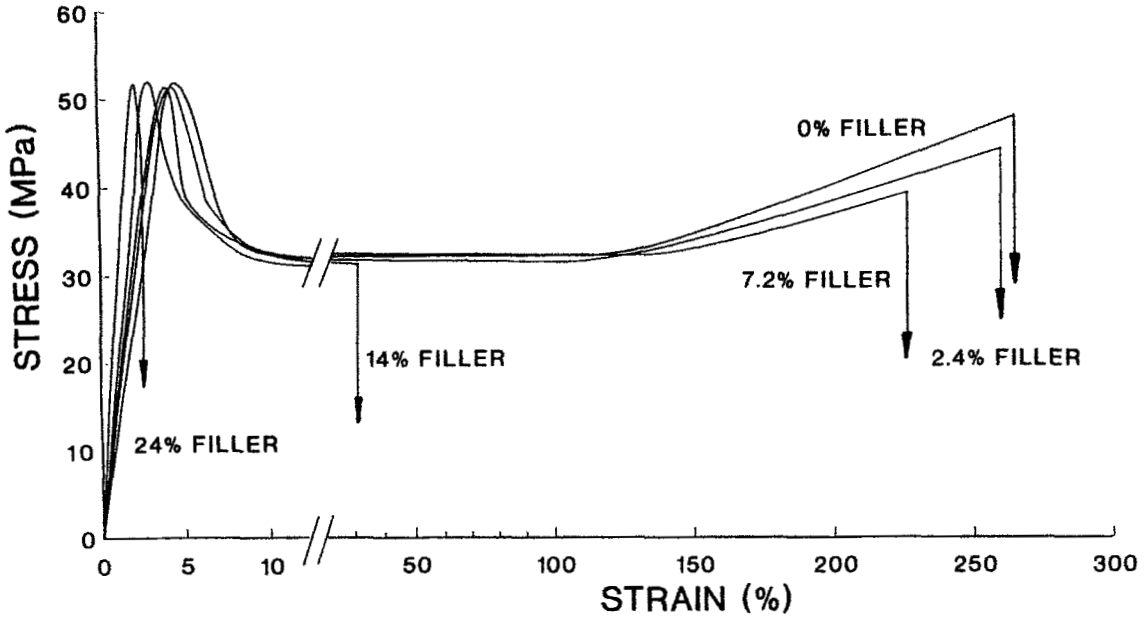

Figure 2 Engineering stress–strain curves for unfilled PETG and four compositions with calcium carbonate filler fractions of 2.4, 7.2, 14, and 24 vol %.

strain. The unfilled polymer reached an engineering strain of approximately 270% before it fractured. The stress–strain curves of the filled materials with the lowest amount of $CaCO_3$, 2.4 and 7.2 vol %, were similar to that of the unfilled polymer, although the fracture strain decreased as the filler content increased. The decrease in fracture strain was primarily due to a decrease in the length of the strain-hardening region.

Qualitatively different behavior was observed with higher filler contents, 14 and 24 vol %. With 14 vol % filler, the fracture occurred during formation of the neck (in one specimen) or in the initial stage of neck propagation (in three specimens). The large decrease in fracture strain and unstable character of neck propagation were symptomatic of transitional behavior. With 24 vol % filler, a yield maximum in the stress–strain curve was also reached; however, just past the yield point, as the engineering stress was decreasing toward the draw stress, the specimens fractured. As a result, the fracture strain was only 4%.

Photographs of two fractured specimens, one with 2.4 vol % filler and the other with 14 vol %, are shown in Figure 3. The specimen with 2.4 vol % filler fractured during strain-hardening after the neck had propagated through the entire gauge section. In contrast, in the specimen with 14 vol % filler, fracture occurred after the neck propagated through less than one-fifth of the gauge length while the remainder of the gauge section was not plastically deformed. Necking initiated in both specimens, while the subsequent stability of the neck defined the transition from ductile to quasi-brittle behavior. With the lower filler content, the neck was stable and propagated through the gauge length. At the higher filler content, the neck formed but it was not strong enough to support drawing, and fracture occurred in the neck. Thus, the ductile-to-quasi-brittle transition was from propagation of a stable neck through the entire gauge length of the specimen to fracture in the neck without propagation.

In all the filled polymers, profuse stress-whitening due to voiding around the filler particles accompanied formation and propagation of the neck. To observe the voids, the drawn region was cryogenically fractured parallel to the draw direction. The micrograph in Figure 4 shows numerous elongated voids that contain filler particles. The voids have the shape that would be expected if the polymer debonded and

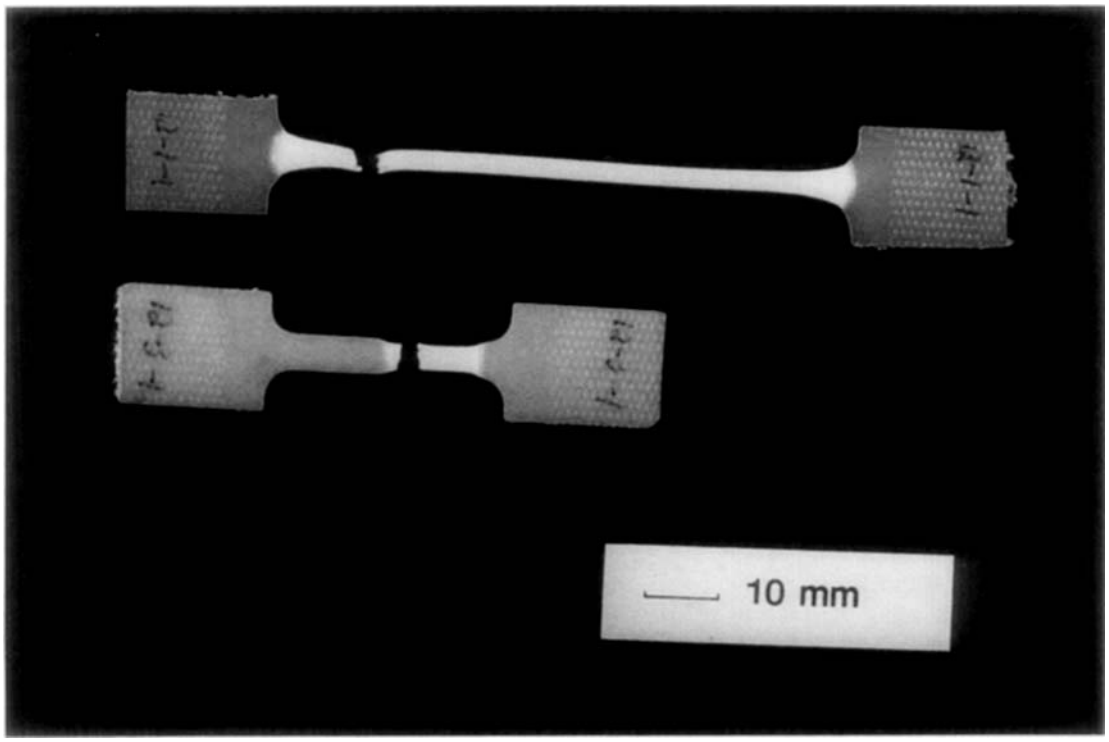

Figure 3 Photographs of two fractured specimens of filled PETG: (upper) 2.4 vol % calcium carbonate; (lower) 14 vol % calcium carbonate.

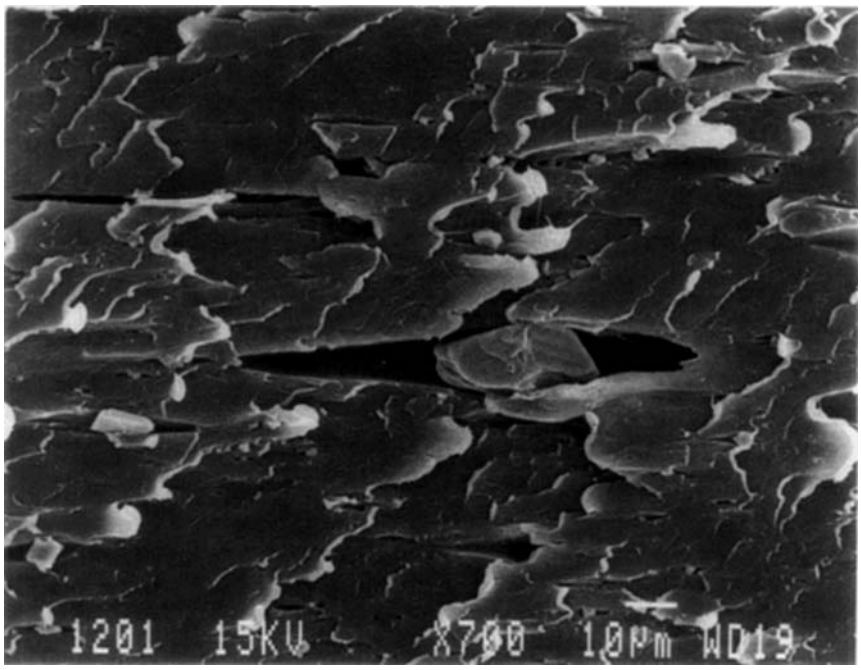

Figure 4 SEM photograph of the neck region of PETG filled with 2.4 vol % calcium carbonate. The neck was cryogenically fractured parallel to the draw direction to show the particles debonded from the matrix. The loading direction was horizontal.

drew out around the particles. Debonding of particles made it possible for the matrix polymer to undergo the large local strain required in the necking process.

Figure 5 illustrates the dependence of the engineering yield stress (upper yield stress), draw stress (lower yield stress), and fracture stress on the filler

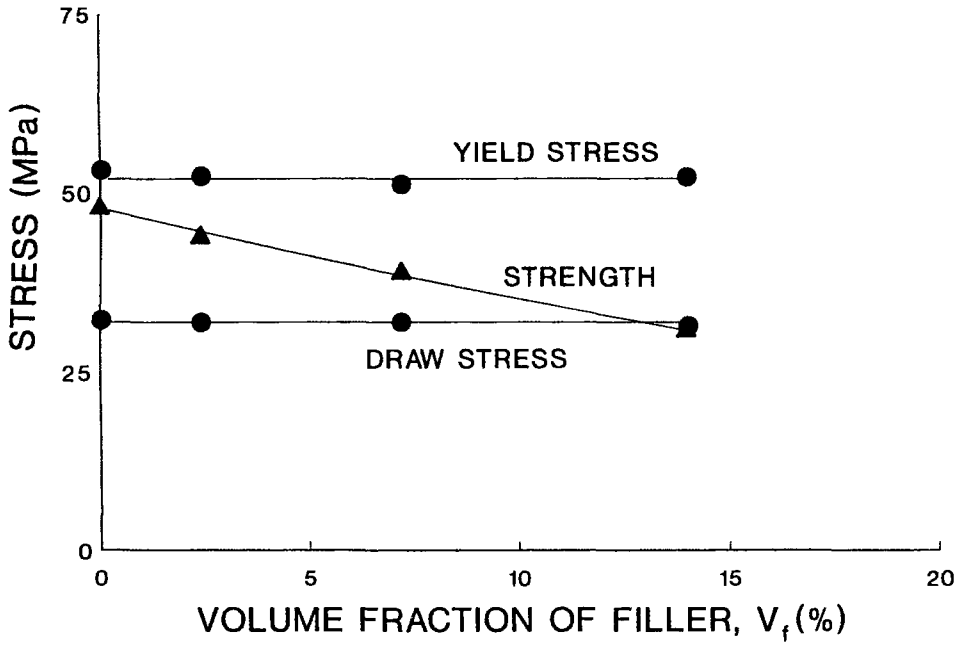

Figure 5 The engineering yield stress, draw stress, and strength of filled PETG plotted against the volume fraction V_f of calcium carbonate.

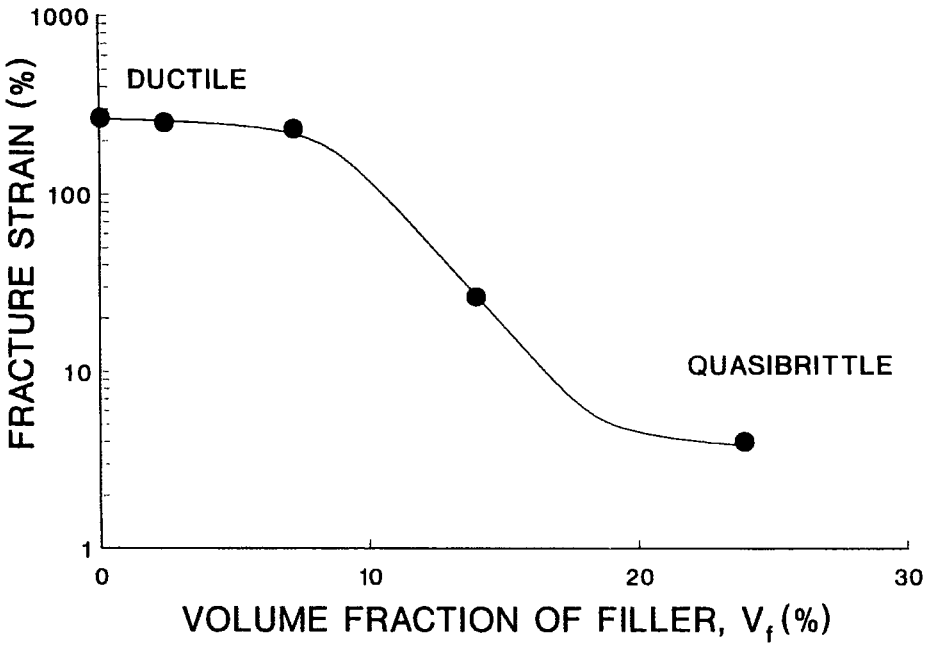

Figure 6 The fracture strain of filled PETG plotted against the volume fraction of calcium carbonate.

volume fraction (V_f). Neither the yield stress nor the draw stress depended on V_f. In contrast, the fracture stress decreased with an increase in the filler content. At low filler contents, the fracture stress was higher than the draw stress due to strain-hardening of the matrix. At V_f = 14 vol %, the fracture stress decreased to the level of the draw stress and a transition from ductile to quasi-brittle behavior occurred.

The engineering strain at fracture is plotted as a function of V_f in Figure 6. Initially, as the filler content was increased to 7 vol %, the fracture strain decreased slightly from 270 to 230% due to a reduction in the strain-hardening region. The fracture strain dropped sharply at roughly 14 vol % filler, and at a filler fraction of 24 vol %, the fracture strain was only 4%. This revealed a transition in fracture mode from ductile to quasi-brittle where the fracture strain in the quasi-brittle region was determined essentially by the strain at yield. The composition with 14 vol % filler exhibited intermediate behavior; a neck formed in this composition but the neck was not stable and fracture occurred at a strain of 25–30% as the neck began to propagate. Compositions with filler fractions lower and higher than 14 vol % were distinctly ductile and quasi-brittle, respectively.

Figure 7 summarizes schematically the observed changes in fracture mode and fracture strain with an increase in the filler content. Three fracture modes were distinguished. At low filler contents, fracture was ductile with propagation of the neck through the entire gauge length of the specimen. Compositions with intermediate filler contents failed during neck propagation. This fracture mode, transitional between ductile and quasi-brittle fracture

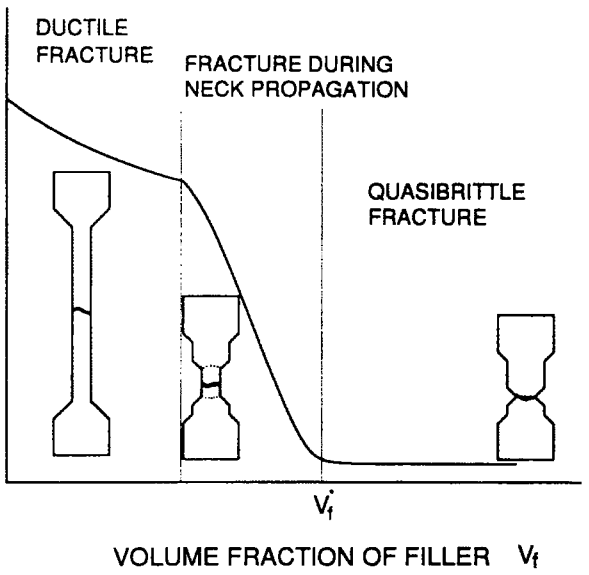

Figure 7 Schematic of the effect of filler content on fracture mode and fracture strain of filled PETG.

modes, has been described for unfilled poly(ethylene terephthalate) (PET) tested at high loading rates.[19] With the highest filler contents, fracture occurred during formation of the neck without propagation.

Ductile-to-Quasibrittle Transition

The observation that the draw stress did not depend on the filler content made it possible to predict the filler volume fraction of the ductile-to-quasi-brittle transition. A strain-hardening material such as PETG is capable of sustaining loads significantly larger than the draw stress. Therefore, the amount of polymer in the cross section can be reduced somewhat, e.g., by the presence of a debonded, nonload-bearing filler, and the polymer will still be able to support the external load without fracturing. However, as the fraction of polymer in the cross section is reduced, a critical point will be reached when the strain-hardening strength of the polymer will not be sufficient to sustain the engineering draw stress.

A simple calculation was made to determine the critical volume fraction of filler at which the engineering draw stress exceeds the strength of the strain-hardened PETG ligaments in the cross section. The filler particles are assumed to be spherical of uniform size and arrayed in a cubic lattice as shown in Figure 8. The largest reduction occurs in the plane that contains the centers of the voids. The ratio of the cross-sectional area of cavities (S_c) to the initial cross section of the specimen (S_0) in this plane is given by

$$S_c/S_0 = \alpha = \beta V_f^{2/3} \tag{4}$$

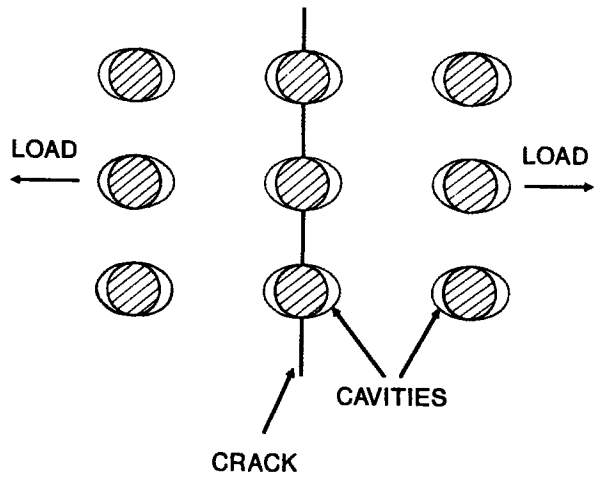

Figure 8 The model of debonded spherical particles arrayed in a cubic lattice used to calculate the critical filler content.

where the geometric factor β for spherical particles is equal to $(9\pi/16)^{1/3} = 1.209$. The fraction of polymer in the plane is then equal to $(1 - \alpha)$. Supposing that the crack propagates through the centers of the cavities and that the ultimate strength of the drawn ligaments between the cavities is the same as that of the unfilled polymer (σ^*), the fracture stress of the filled polymer is the product of the initial fraction of polymer in the cross section and the polymer strength, $(1 - \alpha)\sigma^*$. If this value is higher than the draw stress (σ_d), the neck will be stable and propagate:

$$\sigma_d < \sigma^*(1 - \beta V_f^{2/3}) \tag{5}$$

The fracture mode changes in the case of equality between the two sides of eq. (5). The critical volume fraction of filler (V_f^*) at which this transition occurs is then given by

$$V_f^* = \frac{1}{\beta^{3/2}}\left(1 - \frac{\sigma_d}{\sigma^*}\right)^{3/2} \tag{6}$$

From eq. (6) it is seen that the critical filler volume fraction depends on the ratio of the strength to the draw stress of the polymer. Since this quantity represents the amount of strain-hardening, the critical volume fraction should be strongly dependent on the capacity of the polymer to strain-harden.

The dependence of the critical filler content on the degree of polymer strain-hardening (D), defined as $D = \sigma^*/\sigma_d$, is plotted in Figure 9. If D is close to 1, then V_f^* is close to zero. Hence, if a polymer does not strain-harden, even a small amount of filler will lead to loss of ductility. Initially, the critical volume fraction increases rapidly with degree of strain-hardening, but then it levels off. For PETG, the degree of strain-hardening $D = 1.47$ gives a critical filler content of $\approx$ 14 vol %. The applicability of eq. (6) is limited by the maximum volume fraction of a simple cubic array of spherical particles, and, therefore, eq. (6) is applicable only when the critical volume fraction V_f^* is no greater than 0.52. This corresponds to a value of 4.7 for the maximum degree of strain-hardening.

The generality of eq. (6) is demonstrated for various polymers in Table I. For example, the critical volume fraction calculated from eq. (6) for rigid PVC, which is not strongly strain-hardening, is low, $\approx$ 2.0 vol %. The critical volume fractions for PC and PETG, which are more strain-hardening, are higher, from 10 to 15 vol %. The critical volume fractions for PP and PET are 17 and 27 vol %, re-

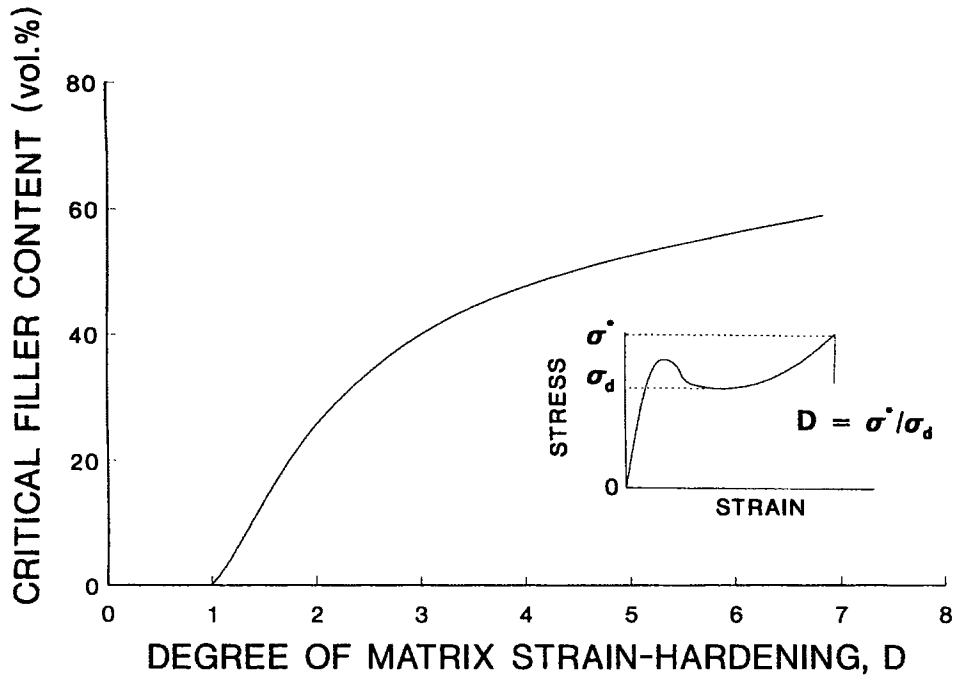

Figure 9 Dependence of the critical volume fraction of filler V_f^* calculated from eq. (6) on the degree of matrix strain-hardening.

spectively; V_f^* for polyethylene (PE), which is easily oriented, is the highest, 16–33 vol %. In all these cases, the degree of strain-hardening is within the applicability of eq. (6). Experimental data show good agreement with the calculated V_f^* values. For example, rigid PVC loses its ductility at filler contents as low as 5 vol %. In filled PP and PET, the transition is observed at V_f^* = 10–15 vol %, and in filled PE, at 20–40 vol %. In general, strain-hardening of polymers increases with molecular weight. This is illustrated with data for PE where the critical volume fraction increases from 20 to 40 vol % when the molecular weight increases from 40,000 to 1,000,000. Data also exist that show a filled rubber with a very high degree of strain-hardening is not brittle up to a filler content of 55 vol %.[16] This observation is consistent with eq. (6) in so far as eq. (6) predicts that if D is large the filled polymer should still be ductile when the filler volume fraction approaches the applicability limit of 0.52. When

Table I Critical Volume Fraction of Filler (%)

Material	σ_y (MPa)	σ_d (MPa)	σ^* (MPa)	ε^* (%)	V_f[a] (Vol %)	V_f[b] (Vol %)	Ref.
PP	44	32.2	51.9	570	17	10–15	6
PETG	53	32.6	48	272	14	14	Fig. 5
PET	50	28	57	530	27	—	19
PVC	60	35	38	90	2	< 5	15
PC	62	47	65–70	120	11–14	—	20
SHMWPE[c]	24	17–19	40	420	29–33	40	14
HDPE[d]	29.6	15	23.4	600–800	16	20	4, 14
PVC rubber						> 55	16

[a] Calculated from eq. (6).
[b] Experimental data.
[c] Molecular weight 1,000,000.
[d] Molecular weight 40,000.

strain-hardening with uniform extension dominates the engineering stress–strain curve, as is the case with most rubbers, the approach embodied in eq. (6) is essentially equivalent to Nielsen's approach.

Draw Strain

Because the stress on the polymer is higher in cross sections that contain particles than in cross sections without, the polymer strain is also higher in cross sections that contain particles. The model used to estimate V_f^* was used to determine the dependence of the draw strain and the fracture strain on the filler volume fraction. Considering again the cubic array of spherical cavities in Figure 10, the strain in section A that contains no cavities will be equal to the strain of the end of the neck propagation region for unfilled polymer (ε_d^0), while the strain in section B, which contains the cavity, will be larger than ε_d^0. To determine the draw strain in section B, the stress–strain relationship of the polymer in the strain-hardening region was approximated by a linear function:

$$\sigma = \sigma_d + E_d(\varepsilon - \varepsilon_d^0) \quad \text{for} \quad \varepsilon > \varepsilon_d^0 \tag{7}$$

where E_d is the slope of the stress–strain curve during strain-hardening. The stress σ_x on the plane at a distance x from the plane passing through the center of the cavity in Figure 10 is given by

$$\sigma_x = \sigma_d \frac{S_0}{S_x} = \sigma_d \left[\frac{a^2}{a^2 - \pi(R^2 - x^2)} \right] \tag{8}$$

where a is the initial length of the element in Figure 10, and S_0 and S_x, the cross-sectional areas of polymer in section A (without the cavity) and at position x in section B, respectively. The additional strain at a position x in section B, $\Delta\varepsilon_x = \varepsilon_x - \varepsilon_d^0$, is then

$$\Delta\varepsilon_x = \frac{\sigma_x - \sigma_d}{E_d} = \frac{\sigma_d \pi(R^2 - x^2)}{E_d[a^2 - \pi(R^2 - x^2)]} \tag{9}$$

Assuming at $V_f \ll 1$ that the term $\pi(R^2 - x^2)$ in the denominator is small compared to a^2, eq. (9) is integrated between $-R$ and $+R$. Dividing the result by the initial length (a), the average additional strain, $\Delta\varepsilon$ (i.e., $\varepsilon_d = \varepsilon_d^0 + \Delta\varepsilon$), is given by

$$\Delta\varepsilon = \frac{1}{a}\int_{-R}^{R} \frac{\sigma_d \pi(R^2 - x^2)}{E_d a^2}\, dx = \frac{4\pi R^3 \sigma_d}{3a^3 E_d} \tag{10}$$

Since $4\pi R^3/(3a^3) = V_f$, the draw strain of the filled polymer, ε_d, is

$$\varepsilon_d = \varepsilon_d^0 + \frac{\sigma_d}{E_d} V_f \tag{11}$$

where ε_d^0 is the draw strain for the unfilled polymer. The draw strain calculated from eq. (11) for filled PETG is plotted in Figure 11 using values of σ_d = 32.6 MPa, ε_d^0 = 1.37, and E_d = 11.5 MPa. The draw strain of PETG should increase by about 7 and 20% for filler contents of 2.4 and 7.2 vol %, respectively. The draw strains for these two compositions were estimated from the engineering stress–strain

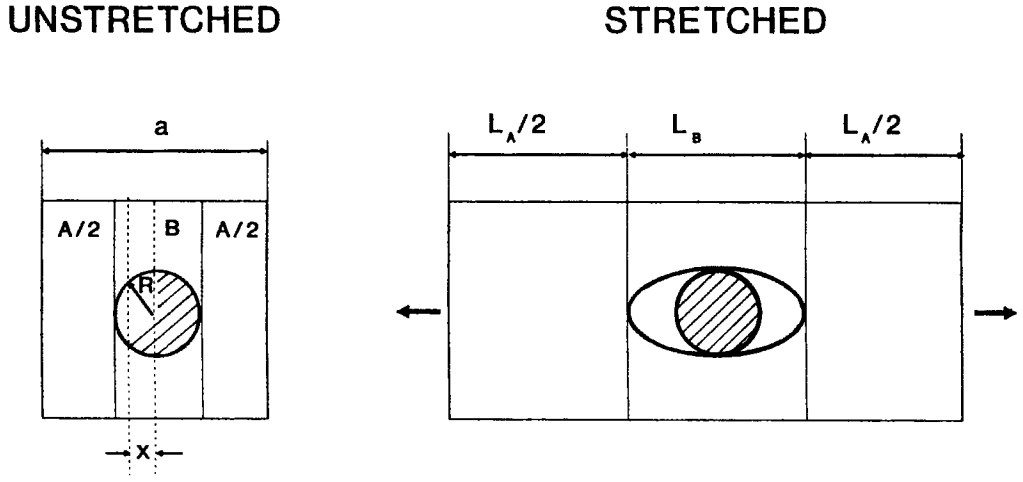

Figure 10 The model used to determine the draw strain and fracture strain. R is the particle diameter; a, the dimension of the cubic lattice; and x, the distance from the center of the spherical filler particle.

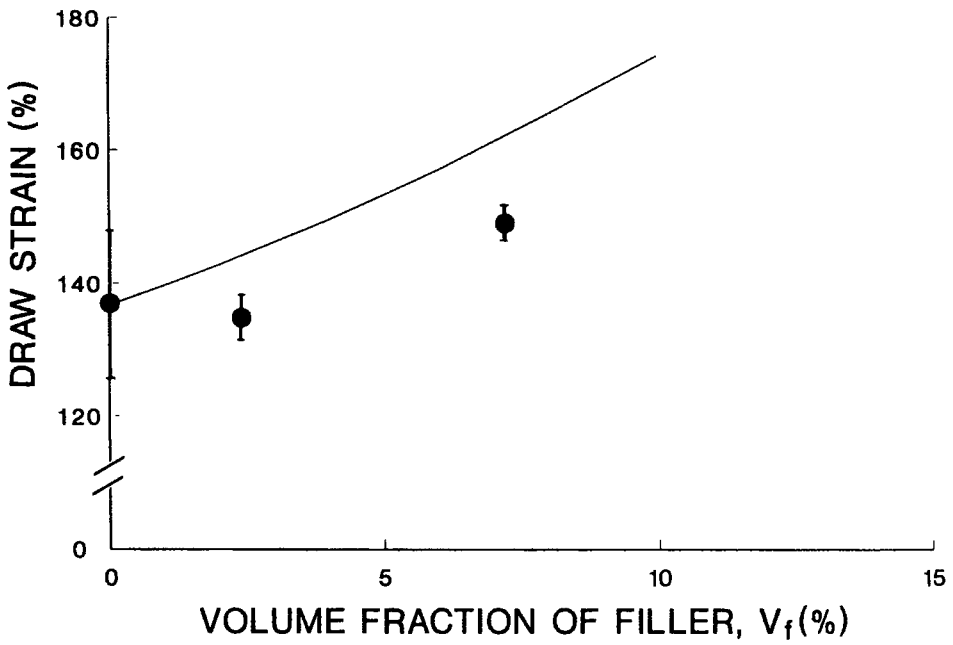

Figure 11 The draw strain of calcium carbonate-filled PETG compared with the prediction from eq. (11) plotted against volume fraction of filler, V_f.

curve and are included in Figure 11 for comparison. Within the scatter of the data, there was no significant difference between the draw strain of PETG and PETG with 2.4 vol % filler; however, as predicted, there was a significant increase in draw strain with 7.2 vol % filler.

Strain at Fracture

A similar analysis can be made of the ductile fracture strain. Fracture occurs when the strain in a plane passing through the center of the cavities reaches the fracture strain of the unfilled polymer. The stress–strain relationship of the polymer in the strain-hardening region is given by eq. (7), which, for convenience, can be rewritten as

$$\sigma = \sigma^* - E_d(\varepsilon^* - \varepsilon) \quad \text{for} \quad \varepsilon_d^0 < \varepsilon < \varepsilon^* \qquad (12)$$

where σ^* and ε^* are the fracture stress and strain of the unfilled polymer. Combining eqs. (3) and (12), the strain in section A in Figure 10 when fracture occurs is given by

$$\varepsilon_A = \varepsilon^* - \beta\sigma^* V_f^{2/3}/E_d \qquad (13)$$

The length of section A (L_A) is then given by the strain multiplied by the original length of the section, $a - 2R$:

$$L_A = (\varepsilon^* - \beta\sigma^* V_f^{2/3}/E_d)(a - 2R) \qquad (14)$$

In section B, the cross section of polymer in a plane at a distance x from the plane that contains the centers of the cavities is $S_x = S_0 - \pi(R^2 - x^2)$, where $S_0 = a^2$ is the initial cross section and $\pi(R^2 - x^2)$ is the cross section of the cavity. Likewise, the cross section of the plane that contains the centers of the cavities, which is also the plane where fracture occurs, is given by $S_c = a^2 - \pi R^2$. Then, the stress on a plane in section B at fracture is

$$\sigma_x = \sigma^* \frac{S_c}{S_x} = \sigma^* \frac{a^2 - \pi R^2}{a^2 - \pi R^2 + \pi x^2} \qquad (15)$$

Substituting eq. (15) into eq. (12) and assuming the term $\pi(R^2 - x^2)$ in the denominator is small compared to a^2, the polymer elongation in section B is given by

$$\varepsilon_x = \varepsilon^* - \frac{\sigma^* \pi x^2}{E_d a^2} \qquad (16)$$

Equation (16) is integrated between $-R$ and $+R$ to obtain the extension in section B (L_B) at fracture:

$$L_B = 2R\varepsilon^* - \frac{2\sigma^* \pi R^3}{3E_d a^2} \qquad (17)$$

The total length at fracture is the sum of L_A and L_B. Dividing $L_A + L_B$ by the initial length, a, the strain at fracture (ε_f) is given as

$$\varepsilon_f = \varepsilon^* - \frac{\beta\sigma^*}{E_d} V_f^{2/3} + \frac{\sigma^*}{E_d} V_f \qquad (18)$$

The fracture strain calculated from eq. (18) for filled PETG is compared with experiment in Figure 12. For PETG, values of $\beta = 1.2$, $\sigma^* = 48$ MPa, $\varepsilon^* = 2.7$, and $E_d = 11.5$ MPa were used. Equation (18) is meaningful only if the fracture is ductile, i.e., if $V_f < V_f^*$. If $V_f > V_f^*$, Equation (18) gives $\varepsilon_f < \varepsilon_d$, which means that the neck is not stable. This is shown in Figure 12 by a steplike drop in fracture strain at $V_f = V_f^*$. Preceding V_f^*, there may be a transition region where the neck forms and begins to propagate but fractures before it reaches the end of the gauge length. This can occur when the volume fraction is close to V_f^* and the propagating neck encounters a flaw or region of slightly higher filler content that exceeds V_f^*.

The fracture strain predicted by eq. (18) is always lower than that obtained from Nielsen's numerical prediction for debonded particles, which is included in Figure 12 for comparison. However, the most significant difference between Nielsen's curve and the present approach concerns the sharp drop in fracture strain at the critical filler volume fraction V_f^*. Only the present approach is able to accommodate this particle-induced transition from propagation of a stable neck through the specimen to fracture in the neck without propagation. A second difference is related to the material parameters that determine the fracture elongation. According to Nielsen, these parameters are only the filler content and the fracture strain of the unfilled polymer. In the approach embodied in eq. (6), the fracture mode also depends on the strain-hardening characteristics of the polymer. Generally, the strain-hardening of a polymer increases with its molecular weight. Consequently, it is natural to expect that increasing the molecular weight will improve the ductility of filled polymers. Finally, eq. (6) was developed specifically for polymers that undergo localized deformation by necking and drawing with subsequent strain-hardening. For polymers that undergo uniform extension with very high strain-hardening, such as rubbers, the critical filler content is very high and the fracture strain behavior becomes similar to that predicted by Nielsen.

CONCLUSIONS

Previous approaches of Smith and Nielsen for predicting the failure behavior of filled polymers were extended to polymers that deform by necking and

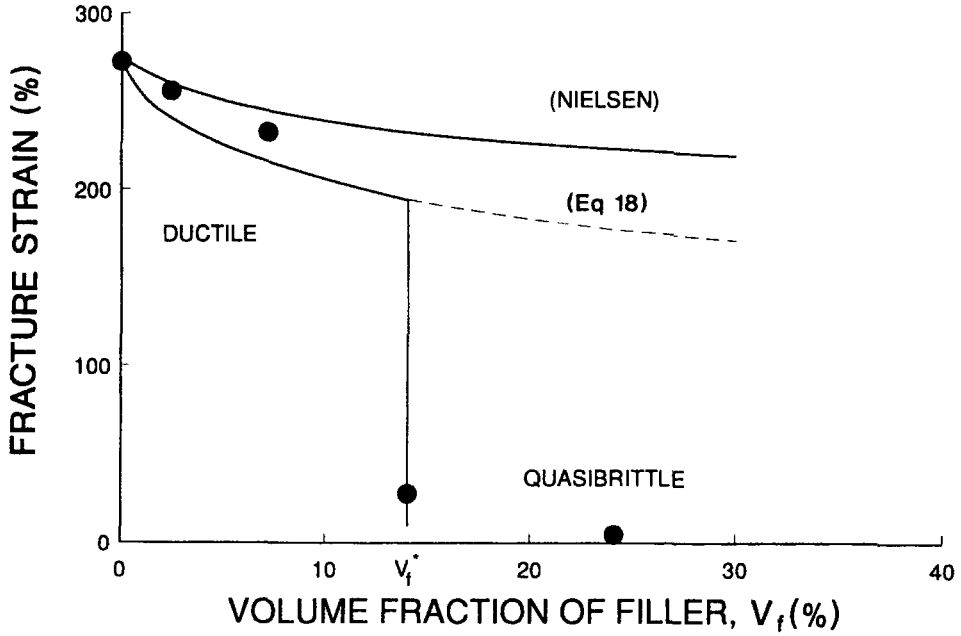

Figure 12 The fracture strain of calcium carbonate-filled PETG compared with the prediction from eq. (18) and Nielsen's numerical solution for debonded particles.[18]

drawing. By assuming that stable neck propagation depends on the strain-hardening strength of the polymer ligaments between debonded particles, a simple model was used to predict the dependence of fracture strain on filler volume fraction. The results were compared with data for a calcium carbonate-filled copolyester. The study led the following conclusions:

1. A sharp drop in fracture strain occurs at a critical volume fraction of filler due to a change in fracture mode from propagation of the neck through the entire gauge length to fracture in the neck without propagation.
2. The critical volume fraction at which the fracture mode changes from ductile to quasi-brittle is determined primarily by the degree of polymer strain-hardening.
3. When the fracture mode is ductile, the fracture strain should decrease gradually, and the draw strain should increase gradually, with increasing filler content.
4. Predictions show reasonable agreement with data for a calcium carbonate-filled copolyester and with data in the literature for other filled polymers that deform by necking and drawing.

The authors gratefully acknowledge the generous financial support of the Army Research Office (DAAL03-88-K-0097) and the NASA Center for the Commercial Development of Space on Materials for Space Structures.

REFERENCES

1. L. Nicolais and M. Narkis, *Polym. Eng. Sci.*, **11**, 194 (1971).
2. O. Ishai and L. J. Cohen, *J. Compos. Mater.*, **2**, 302 (1968).
3. K. Friedrich and U. A. Karson, *Fibre Sci. Technol.*, **18**, 37 (1983).
4. V. A. Tochin, E. N. Shchupak, V. V. Tumanov, O. B. Kulachinskaya, and M. I. Gai, *Mech. Comp. Mater.*, **20**, 440 (1984).
5. N. S. Enicolopian, M. L. Friedman, I. O. Stalnova, and V. L. Popov, *Adv. Polym. Sci.*, **96**, 1 (1990).
6. S. N. Maiti and B. H. Lopez, *J. Appl. Polym. Sci.*, **44**, 353 (1992).
7. G. Mikhler, Yu. M. Tovmasian, V. A. Topolkaraev, I. L. Dubnikova, and V. Shmidt, *Mech. Comp. Mater.*, **24**, 167 (1988).
8. K. Kendall, *Br. Polym. J.*, **10**, 35 (1978).
9. B. Pukanszky, F. Tudos, J. Jankar, and J. Kolarik, *J. Mater. Sci. Lett.*, **8**, 1040 (1989).
10. P. Bajaj, N. K. Jha, and R. K. Jha, *Polym. Eng. Sci.*, **29**, 557 (1989).
11. M. Sumita, Y. Tsukumo, K. Miyasaka, and K. Ishikawa, *J. Mater. Sci.*, **18**, 1758 (1983).
12. K. Mitsuishi, S. Kodama, and H. Kawasaki, *Polym. Eng. Sci.*, **25**, 1069 (1985).
13. B. Pukanszky, B. Turcsanyi, and F. Tudos, in *Interfaces in Polymers, Ceramic and Metal Matrix Composites, Proceedings of the Second International Conference on Composite Interfaces*, H. Ishida, Ed., Elsevier, New York, 1988, p. 467.
14. V. A. Topolkaraev, Yu. M. Tovmasian, I. L. Dubnikova, A. I. Petrosian, I. N. Meshkova, A. A. Berlin, Yu. P. Gomza, and V. V. Shilov, *Mech. Comp. Mater.*, **23**, 419 (1987).
15. W. Rovatti and E. G. Bobalek, *J. Appl. Polym. Sci.*, **7**, 2269 (1963).
16. T. L. Smith, *Trans. Soc. Rheol.*, **3**, 113 (1959).
17. L. E. Nielsen, *J. Compos. Mater.*, **1**, 100 (1967).
18. L. E. Nielsen, *J. Appl. Polym. Sci.*, **10**, 97 (1966).
19. D. L. Wilfong, A. Hiltner, and E. Baer, *J. Mater. Sci.*, **21**, 2014 (1986).
20. *Encyclopedia of Polymer Science and Engineering*, Wiley, New York, 1988, Vol. 11, pp. 656–658.

Received September 15, 1992
Accepted November 22, 1992